Numerical and experimental studies of compression-tested copper, mortar contact method

Gabriel Jesús Torrente-Prato

Departamento de Mecánica, Universidad Simón Bolívar, Caracas, Venezuela, gtorrente@usb.ve

Abstract
Simulation of compression test of copper is made with the mortar contact method and assuming: axial symmetry, multiple point constraint of type plane, concentrate load and coulomb friction. Copper is simulated like isotropic material, elastic until it yields stress, and then like a hardening material with incremental plasticity. Copper behavior was calculated from experiments. Seventeen compression tests without lubrication were carried out to cylindrical samples at room temperature. The Stress vs. Strain relationship was calculated using two friction corrections; the Rowe Correction and the Dieter Correction. It was concluded that the simulation made with the mortar contact method and the Dieter Correction is a good alternative to simulate the compression test, being the differences between the simulation and the experiments lower than 7.33%, the hypothesis of axial symmetric does not keep away the simulation of the reality and new numerical analysis will allow the development of better friction corrections.

Keywords: Compression test; barreling; copper; finite element; mortar contact; friction.

Estudio numérico y experimental del ensayo de compresión del cobre, método de contacto mortar

Resumen
La simulación del ensayo de compresión del cobre se realizó con el método de contacto con mortero y asume: simetría axial, restricción de puntos múltiples de tipo plano, carga concentrada y fricción coulombiana. El cobre se simula como material isotrópico, elástico hasta fluencia, y luego como un material endurecible con plasticidad incremental. El comportamiento del cobre se calculó a partir de experimentos. Se realizaron diecisiete ensayos de compresión sin lubricación a muestras cilíndricas a temperatura ambiente. La relación Esfuerzo vs. Deformación se calculó usando dos correcciones por fricción; La Corrección de Rowe y la Corrección Dieter. Se concluye que: la simulación realizada con el método de contacto con mortero y la Corrección Dieter es una buena alternativa para simular la prueba de compresión, siendo la diferencia entre la simulación y los experimentales inferior a 7,33%, la hipótesis de simetría axial no aleja la simulación de la realidad y nuevos análisis numérico permitirán el desarrollo de mejores correcciones por fricción.

Palabras clave: Ensayo de compresión; abarrilamiento; cobre; elemento finito; contacto de mortero; fricción.

1. Introduction

Massive metal forming processes deform the piece to compression. Some examples of these processes are: rolling, extrusion, and forging. [1]

The simulations had allowed clarifying the behavior of metals during the industrial processes of forming.

The friction between the piece and the tool is one of the most important variables that affect the forming process. The frictional force not only determines the forming load, but it also influences the workpiece quality. [2] The first step in simulating the friction is to define the contact pair. In this paper the contact pair type mortar contact was assessed.

Mortar contact is a simple and consistent formulation method. [3] It is a surface-to-surface method which usually leads to better convergences and a more uniform stress field. [4]

The contact pair will define the type of friction between the faces. Generally the friction is classified into three types:

quasi-static dry friction; dynamic and sliding friction; and wear and plowing. [5]

A friction mechanism of type II was used for this study, dynamics and sliding friction.

Dynamic and sliding friction describes, principally, two friction mechanisms: Dry sliding friction of metallic bodies and Stick-slip motion. [5] In this work we used the first one.

Dry sliding friction or Coulomb friction takes: the compressive normal force N and the coefficient of friction μ, to obtain the friction force F. [5]

Mortar contact method has been studied by many authors.

Christian Weißenfels et al. [6] in 2015 proposed a new contact element, and for the discretization of the new contact element the Mortar method was chosen

Tod Laursen et al. [7] in 2012 published a study on the last 15 years of Mortar Contac method. The study shows how this method has improved since a basic summary of the mortaring idea to the extension of these methods to large deformation, large sliding, and the newest results where it can be extended to a much broader class of interface mechanics applications.

Bin Yang et al. [8] in 2005 presented the results of their studies on the mortar contact methods for large deformation with frictional sliding. They concluded that the mortar method has shown to preserve optimal convergence rates in tied contact problems.

Thiago Doca et al. [9] in 2014 introduced a new approach based on a mortar formulation and the enforcement of contact constraints. Their conclusion centered on the accuracy and efficiency of the approach against the traditional node-to-segment penalty contact formulation.

This paper presents the simulation of compression testing using the Mortar Contact method. It was concluded that the aforementioned method allows describing to a great extent the compression test, being the maximum differences between the simulation and the experiments 7.33 %.

The novelty of this paper evolves around the importance of applying the multiple point constraint of type plane condition. This condition avoids the Flash in the sample. The Flash effect is observed, for example, on friction welding.

2. Experimental procedure

The copper was characterized by atomic emission spectroscopy with the Spectro LAb Junior and with metallographic microscope. The characterization showed a 99.9 % purity in copper with an average grain size of 80 ☐m.

Seventeen compression tests were performed without lubrication, with a speed of 0.028 mm/s, and an acquisition rate of 175 data per second. Compression tests were performed according to the specifications of ASTM E 9-09A [10] with the universal testing machine MTS-312.31/227. The copper samples were of 12.6 mm of diameter and 20 mm of height.

The displacement of the load cylinder of the testing machine was the variable. The first compression test was made up until a displacement of 2 mm was achieved, thus causing the displacement to increase up until reaching 14mm during the last test.

Fig. 1 is a photo of some samples tested.

Figure 1. Photos of samples tested, the first is the standard sample, and the following were compressed with loads of 4160, 4878, 5878, 7050, 8771, 11530 and 16067 Kgf. (tests 2, 4, 7, 9, 11, 14, 16 in the Figs. 2 and 3). Source: The author.
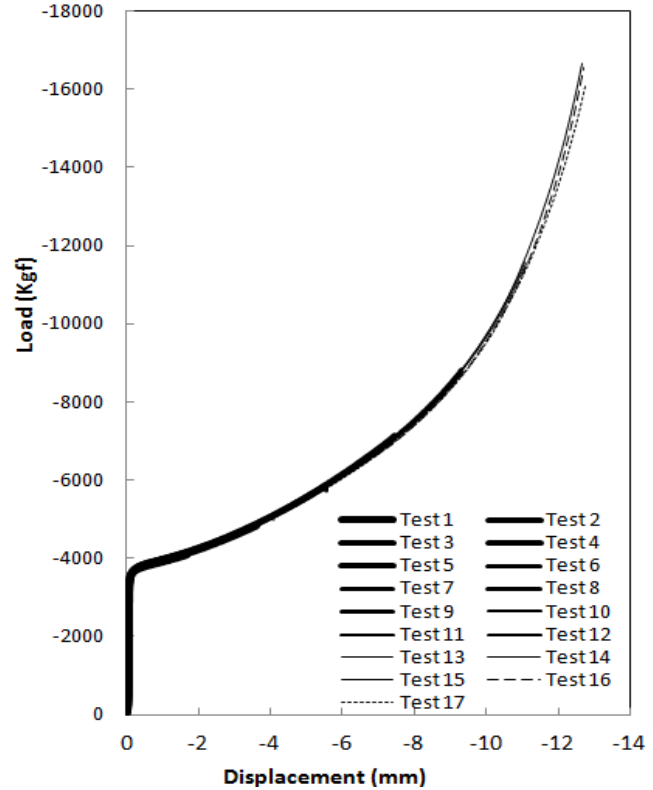

Figure 2. Load vs. Displacement of the seventeen compression tests. Source: The author.

The diagrams of Load vs. Displacement are shown in Fig. 2 and the lengths measured and where they were taken (Fig. 7) on the specimens obtained from these tests are showed with points in the Figs. 8, 9 and 10.

The Stress and Strain were calculated with the following Equations:

$$\sigma_i = \frac{L_i}{A_i} \tag{1}$$

$$\varepsilon_i = Ln\left(\frac{A_0}{A_i}\right) \tag{2}$$

$$h_0 A_0 = h_i A_i \tag{3}$$

$$h_i = h_0 + \Delta l_i \tag{4}$$

Where σ_i is the instant stress, ε_i is instant strain, L_i is the instant load, h_0, A_0, h_i and A_i, are the initial height, initial area,
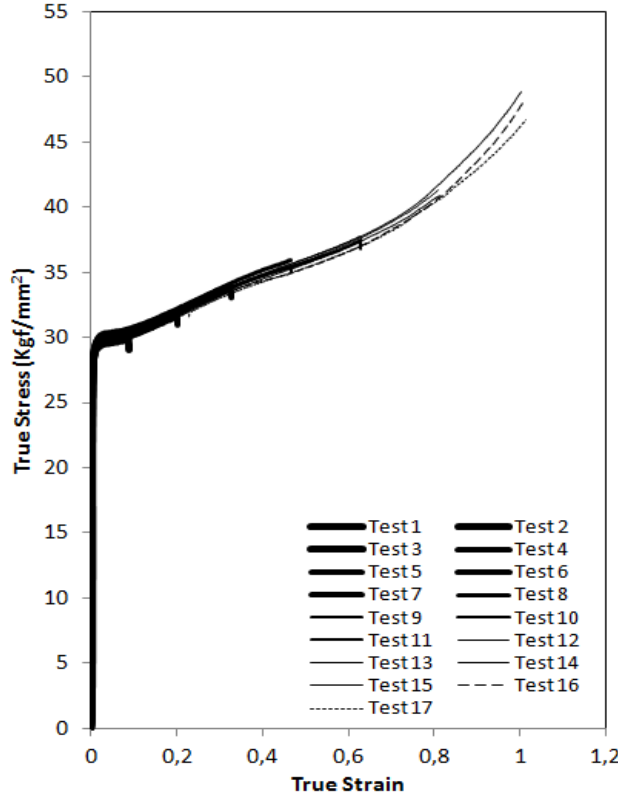
Figure 3. Stress vs. Strain diagrams of the seventeen compression tests calculated with the volume conservation principle.
Source: The author.

instant height and instant area of the sample, respectively; Δl_i is the displacement, and the instant area A_i is calculated with the volume conservation principle (Eq. 3).

Fig. 3 shows the diagrams of Stress and Strain of the seventeen tests, calculated with Equations 1 to 4.

Fig. 2 shows the superposition of all the curves of the seventeen tests.

The superposition of all the curves is in the Fig. 3 too.

The superposition of all curves in Figs. 2 and 3 show the repetitiveness of the tests.

Two friction corrections are used to obtain an approximation for the copper behavior in compression. The Rowe Correction can be written as Eq. 5 [11] and the Dieter Correction as Eq. 6 [12], these relationships are, respectively:

$$\sigma = \frac{\sigma_z}{\left(1 + \dfrac{2f}{3\sqrt{3}}\dfrac{r_i}{h_i}\right)} \tag{5}$$

$$\sigma = \frac{C_f^2 \sigma_z}{2\left[\exp\left(C_f\right) - C_f - 1\right]} \tag{6}$$

Where r_i is the instantaneous values of radius, calculated from A_i (Eq. 3), σ and σ_z (σ_z is σ_i in Eq. 1) are the Equivalent axial stresses without and with the frictional condition (these lasts ones

are took from Fig. 3); f is the Tresca Friction Coefficient and it is Equal to $f = \sqrt{3}\mu$, C_f is the Coulomb stress distribution and is $C_f = 2\mu r_i / h_i$. These Equations are for cylindrical sample and they assume that the barreling is negligible; σ and σ_z are constants throughout the sample height. [13]

The friction coefficient between copper and steel has been estimated on 0.53 for static friction and 0.29 for sliding friction. [14] Figs. 4 and 5 show the results of friction corrections for a bigger range of fiction coefficients.

Fig. 4 shows diagrams of Stress vs. Strain of the test 16 and those obtained with Rowe Correction (Eq. 5).

Fig. 5 shows the diagrams of Stress vs. Strain of test 16 and those obtained with Dieter Correction (Eq. 6).

Figs. 4 and 5 show that while the lower the friction coefficient value is, the stresses obtained with the frictional condition will be closer to the stresses calculated without this condition, but when higher values of friction coefficient are supposed, the real strength of the material will be lower.

3. Numerical simulation

The mesh was made with Gmsh [15] and the simulation was made with Calculix [4], both are open softwares. The simulation was carried out with a HP Pavilion dv6.

The control volume of the simulation is the middle bottom of the sample and the bottom dice (see Fig. 6). This is because we took the hypothesis of axial symmetry, the behavior of the top side is the same as its bottom side.
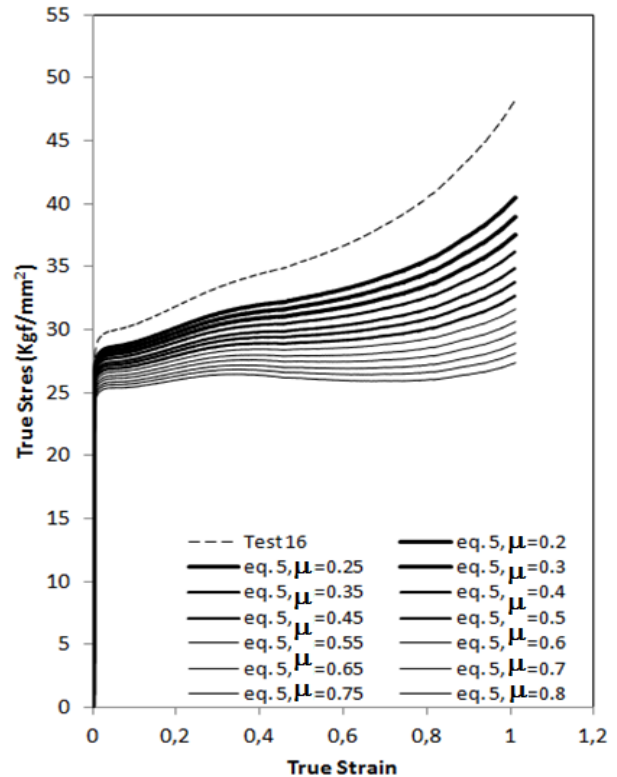

Figure 4. Stress vs. Strain calculated with the Rowe Correction to test 16.
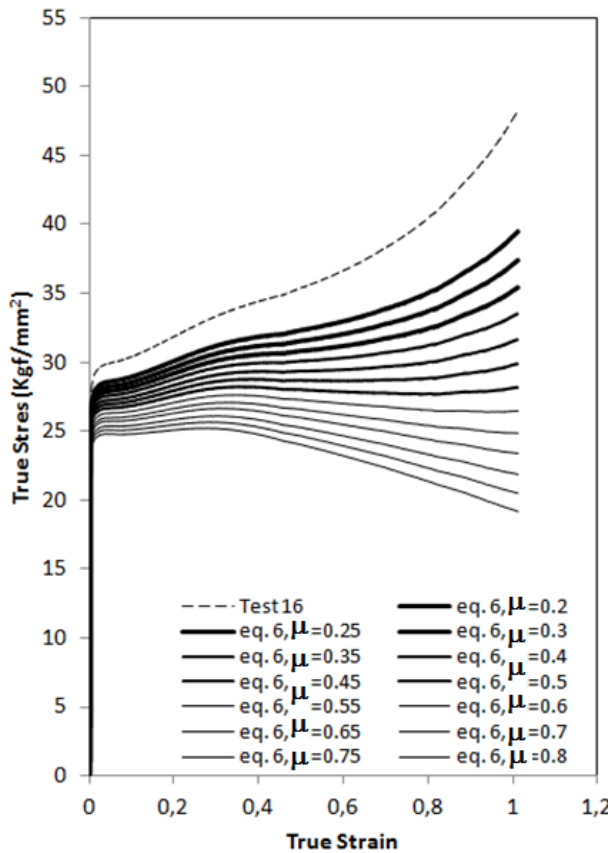Source: The author.

Figure 5. Stress vs. Strain calculated with the Dieter Correction to test 16.
Source: The author.

Rasta *et al*. [16] in 2011 measured experimentally that symmetry in compression test. Chen *et al*. [17] and Raja *et al*. [18] used that symmetry like a boundary condition in their numerical simulations.

Two solids were defined: the first one is for the dice and the second is for the copper samples.

The dies of the universal testing machine are and were simulated like tempered steel AISI-4140, and its behavior, in the load range, is isotropic linear elastic. This behavior is described by the Young Modulus (E) and the Poisson Coefficient (ν), [19] being the Young Modulus 22000 Kgf/mm^2 [20] and the Poisson Coefficient 0.29 [21].

The copper sample was modeled like an isotropic material with linear elastic behavior until the yield stress; and then an incremental plasticity material with hardening. [22] The Young Modulus and a Poisson Coefficient are 11000 Kgf/mm^2 [20] and 0.34 [21], respectively. The plastic behavior is described by the Von Misess Stress (σ_{VM}) and the Equivalent Strain (ε_P). This plastic behavior was calculated by three different ways.

The first one takes the mechanical behavior from the volume conservation principle (test 16 in Fig. 3). The results of this simulation are shown in the Fig. 8.

The second and third simulations take the mechanical behavior from the Eq. 5 (Rowe Correction) and Eq. 6 (Dieter Correction), respectively, (see Figs. 4 and 5). The results of these simulations are shown in the Figs. 9 and 10.

The simulation has boundary conditions in three surfaces: (see Fig. 6)

a) The surface of middle of the copper sample. This surface is free to move and over it a compression load is applied that goes from 0 to 16000 Kgf. This load is simulated like a concentrate load, 222 Kgf for each 72 nodes of this surface, giving approximately a total load of 16000 Kgf (see Fig. 6). Another condition on this surface is the multiple point constraint of the type plane (MPC-PLANE). This MPC-PLANE specifies that all nodes in this surface should stay in a same plane. Note that this plane can move during deformation, depending on the motion of the defining nodes. [4] This last condition avoids ribbon of metals in this surface. This defect of ribbon is also called as Flash (see Fig. 11.c).

b) The bottom surface of the copper sample. This surface is free to move and it was defined to complete the contact pair with the top of the bottom die, mortar contact with coulomb friction.

c) The top surface of the bottom dice. This surface has no freedom degrees, and it was defined to complete the contact pair with the bottom surface of the copper sample.

Fig. 7 shows where the experimental measures were taken; Figs. 8, 9 and 10 show these measures and simulation results.
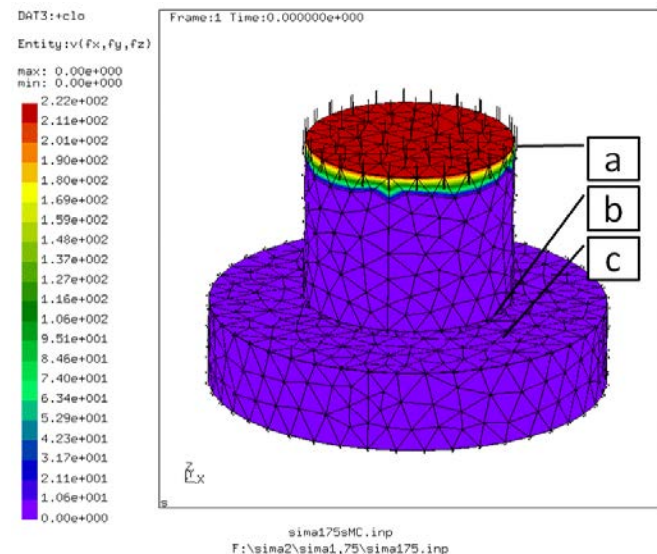

Figure 6. Boundary Condition: (a) The surface of middle of the sample, (b) The bottom of the sample, (c) The top of the lower dice.
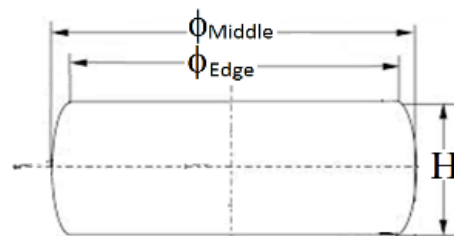Source: The author.

Figure 7. Measurements of the sample: H: height, ϕ_{Middle}: diameter in the middle, and ϕ_{Edge}: diameter in the edges.
Source: The authors.

Fig. 8 shows the simulation results assuming the mechanical behavior of copper obtained directly from principle of volume conservation without any friction correction (Fig. 3).

Fig. 9 shows the simulation results assuming the mechanical behavior of copper obtained with the friction correction of Rowe (Fig. 4).

Fig. 10 shows the simulation results assuming the mechanical behavior of copper as it was obtained with the friction correction of Dieter (Fig. 5).

The simulation shows the behavior inversely proportional of friction with the edge diameter (green lines in the Figs. 8, 9 and 10), nevertheless this effect decreases from Figs. 8 to 10. The middle diameters (brown lines in the Figs. 8, 9 and 10) and the heights (blue lines in the Figs. 8, 9 and 10) have the same behaviors but they are less affected by the friction.

The simulation made with the Dieter Correction (Fig. 10) is the nearest to the experimental measures, with friction coefficients between 0.2 and 0.3. A friction coefficient of 0.3 gives better results for small displacements, being the diameters on the edge and on the middle the same as that of the diameters experimentally measured and a difference between heights of 7.33%, but for bigger displacements a friction coefficient of 0.2 gives better results, being the height the same as that of the height experimentally measured and a difference between the diameters calculated and measured below 5.70%.
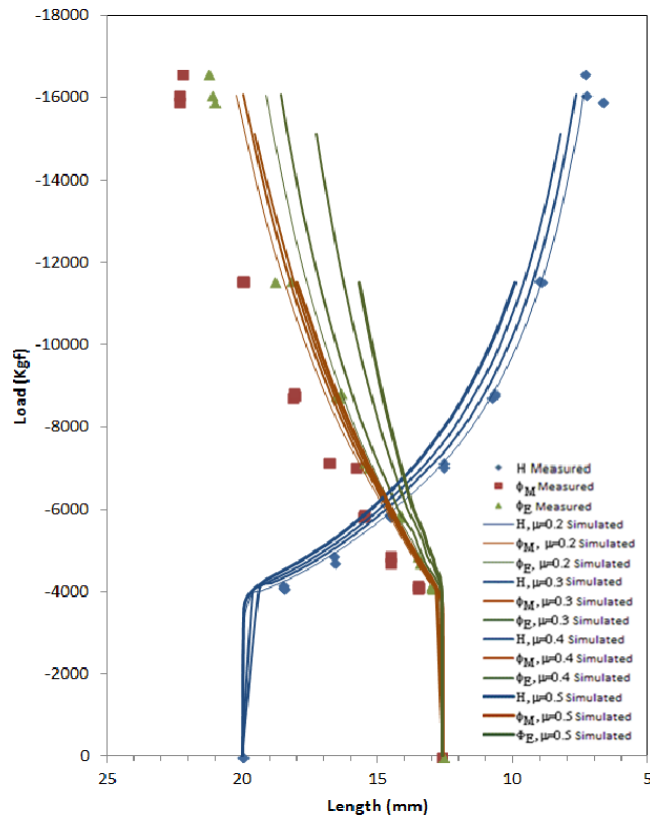

Figure 8. Load vs. Length. The experiments are points and the simulations are lines. The simulation made with different friction coefficients takes the mechanical properties of copper calculated with the volume conservation and without friction correction.
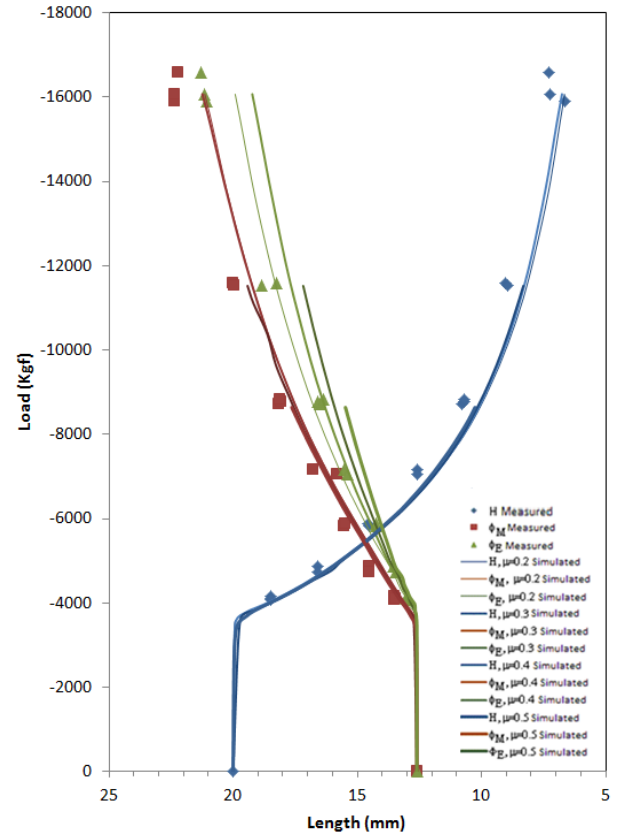Source: The author.

Figure 9. Load vs. Length. The experimental measures are points and the simulations are lines. The simulation made with different friction coefficients takes the mechanical properties of copper calculated with the volume conservation and Rove Correction.
Source: The author.

Fig. 11.a shows the stress on Z for a load of -5878 Kgf.

Fig. 3 shows that the test 7 (Fig. 1), was compressed with a load of -5878 Kgf, Equivalent to 33.75 Kgf/mm^2 (see Fig. 4). This stress for this load (Fig. 11.a) is in the point (a). This was expected because the instant areas were calculated with the volume conservation principle.

Fig. 11.b shows the stress on X for a load of -5878 Kgf. The stress on X is zero in the middle of the sample; this is one of the hypotheses searched with boundary conditions in this surface.

Fig. 11.c shows the displacement on Z for a load of -5878 Kgf without MPC-Plane condition. The Fig. 11.c shows the Flash on the top.

Fig. 12.a shows the stress on Z for a load of -16000 Kgf.

Figs. 11.a and 12.a show that for loads of -5878 and 16000 Kgf, the stresses on Z in the middle of the sample (the tops in the Figures) gave approximately 29.5 and 39.5 Kgf/mm^2, respectively, see point (b) in Fig. 11.a. These values of stresses for these loads are similar to the obtained with the Dieter Correction, 30.34 and 39.47 Kgf/mm^2. Therefore the mechanical behavior obtained with the Dieter Correction is nearer to the reality than the Rowe Correction.
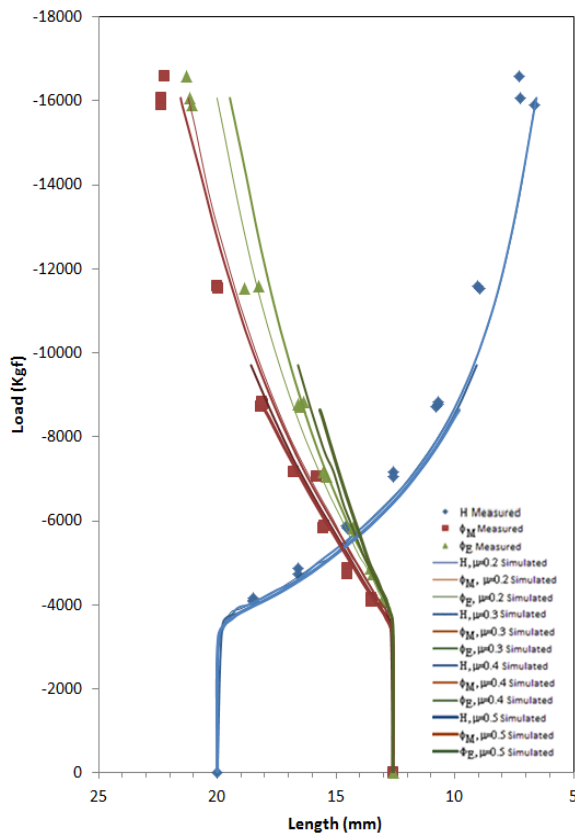
Figure 10. Load vs. Length. The experiment measures are points and the simulations are solid lines. The simulation made with different friction coefficients takes the mechanical properties of copper calculated with the volume conservation and Dieter Correction.
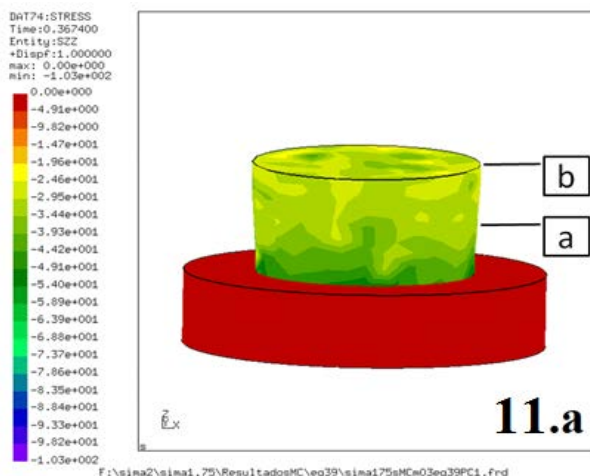Source: The author.

stresses. This would make it possible to define new and better friction correction and improve the simulations of forming processes.

Fig. 13 show the validation of the mesh. The most refined mesh with convergent results is one with an element size factor of 1.75.

4. Conclusions

The Dieter Correction and Rove Correction show that while the lower the friction coefficient value is, the stresses obtained with the frictional condition will be closer to the stresses calculated without this condition, but when higher values of friction coefficient are supposed, the real strength of the material will be lower.

The hypothesis of axial symmetry, that the behavior on the top side is the same as on the bottom side, does not make the simulation move away from the reality.
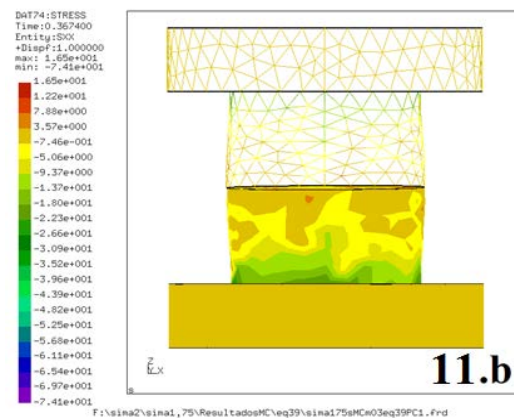

Figure 11.b. Stress on X (Kgf/mm^2). Dieter Correction is assumed, $\mu=0.3$ and the L=-5878 Kgf (16000*0.3674).
Source: The author.

Figure 11.a. Stress on Z (Kgf/mm^2). Dieter Correction is assumed, $\mu=0.3$ and the L=-5878 Kgf (16000*0.3674).
Source: The author.

A better knowledge on the barreling during compression of cylindrical samples will enable predicting the behavior of the sample diameter. That will enable obtaining the instant area in the middle of the sample and calculate the true
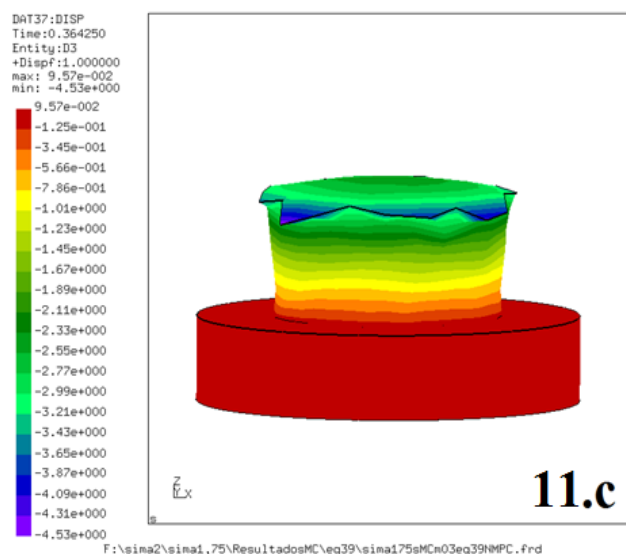

Figure 11.c:.Displacement on Z (mm). Dieter Correction is assumed, $\mu=0.3$ and the L=-5878 Kgf (16000*0.3674).
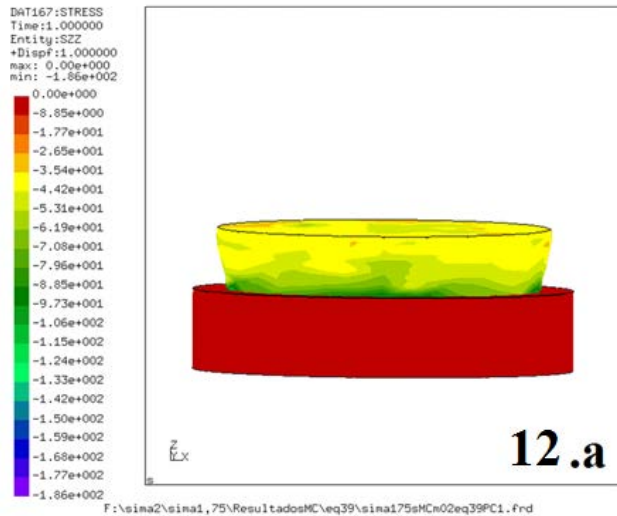Source: The author.

Figure 12.a. Stress on Z (Kgf/mm^2). Dieter Correction is assumed, μ=0.2 and the L=-16000 Kgf (16000*1).
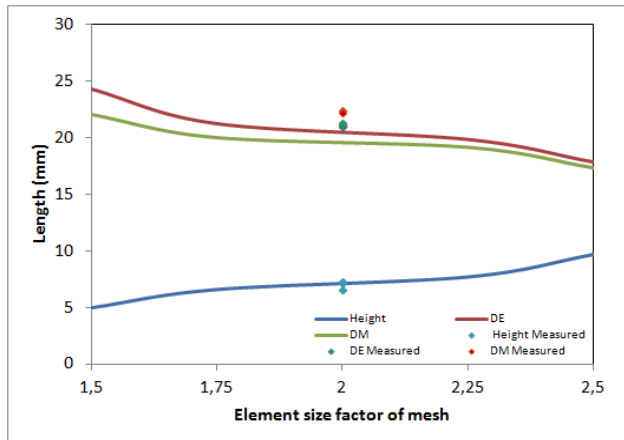Source: The author.

Figure 13. Validation of the mesh. Simulations made with Dieter Correction, μ=0.3 and L= -16000 Kgf.
Source: The authors.

The boundary condition of MPC-Plane in the middle of the sample is necessary to void the flash in the sample when the axial symmetry is a hypothesis in the simulation.

The simulation of the compression test obtained with the Dieter Correction is nearer to the experimental measures than the simulation obtained with the Rove Correction. The differences between the experimental measures and the simulation made with the Dieter Correction are below 7.33%. The Mortar Contact method describes with a good precision the behavior of the copper when it is compressed with open dies.

Numerical analysis on the barreling of the samples during the compression in open dies will allow the development of better friction corrections.

Acknowledgments

References

[1] Kalpakjian, S. y Schimd, S., Manufactura, Ingeniería y Tecnología 5ta edición. Mexico: Pearson, 2008.

[2] Hsua, Y., Yangb, T., Sungc, S. and Changd, Y., Constructing the predictive models of friction coefficient. Materials Science Forum, 505-507, pp. 745-750, 2006.

[3] Hüeber, S., Discretization techniques and efficient algorithms for contact problems, PhD. Thesis, Universität Stuttgart, Germany, 2008.

[4] Dhondt, G., CalculiX CrunchiX USER'S MANUAL [online]. version 2.7., 2014, Available at: www.calculix.de.

[5] Oden, J. and Martins, J., Models and computational methods for dynamic friction phenomena. Computer Methods in Applied Mechanics and Engineering, 52, pp. 527-634, 1985. DOI: 10.1016/0045-7825(85)90009-X.

[6] Weißenfels, C. and Wriggers, P., A contact layer element for large deformations. Computational Mechanics, 55(5), pp. 873-885, 2015. DOI: 10.1007/s00466-015-1140-7

[7] Laursen, T., Puso M. and Sanders, J., Mortar contact formulations for deformable–deformable contact: Past contributions and new extensions for enriched and embedded interface formulations. Computer Methods in Applied Mechanics and Engineering, 205(1), pp. 3-15, 2012. DOI: 10.1016/j.cma.2010.09.006

[8] Yang, B., Laursen, T. and Meng, X., Two dimensional mortar contact methods for large deformation frictional sliding. International Journal for Numerical Methods in Engineering, 62(9), pp. 1183-1225. 2005. DOI: 10.1002/nme.1222

[9] Doca, T., Andrade, F. and Cesar, J., A frictional mortar contact approach for the analysis of large inelastic deformation problems International Journal of Solids and Structures, 51(9), pp. 1697-1715, 2014. DOI: /10.1016/j.ijsolstr.2014.01.013

[10] ASTM E 9-09A, Standard test methods of tensiontesting of metallic materials at room temperature, ASTM Standards, Vols. 03-01, 2010.

[11] Rowe, G., An introduction to the principles of metalworking. London: Edward Arnold, 1965.

[12] Dieter, G., Mechanical Metallurgy 3er Edition. New York: McGraw-Hill, 1986.

[13] Narushima, M., Nakai, T. and Niinomi, M., Advances in metallic biomaterials: Processing and Applications. Sendai: Springer, 2015.

[14] Serway, R. and Jewett, J., Physics for Scientists and Engineers, Volume 1. Belmont: Cengage Learning, 2009.

[15] Remacle, J. and Geuzaine, C., GMSH: A three-dimensional finite element mesh generator with built-in pre- and post-processing facilities. International Journal for Numerical Methods in Engineering, 79(11), pp. 1309-1331, 2009. DOI: 10.1002/nme.2579

[16] Rasti, J., Najafizadeh, A. and Meratian, M., Correcting the stress-strain curve in hot compression test using finite element. International Journal of ISSI, [online]. 8(1), pp. 26-33, 2011. Available at: http://journal.issiran.com/article_6374.html

[17] Chen, Z., Xu, S. and Dong, X., Deformation behavior of AA6063 Aluminium alloy after removing friction effect under hot working conditions. Acta Metallurgica Sinica (English Letters), 21(6), pp. 451-458, 2008.

[18] Raja, R., Lakshminarasimhan, S. and Murugesan, P., Investigation of barreling radius and top surface area for cold upsetting of aluminum specimens. International Journal of Modern Engineering Research, [online]. 3(6), pp. 3852-3862, 2013. Available at: http://www.ijmer.com/papers/Vol3_Issue6/DA3638523862.pdf

[19] Boresi, A., Schmidt, R. and Sidebottom, O., Advanced Mechanics of Materials, 5ed. New York: Wiley, 1993.

[20] Berrocal, L., Elasticidad. Mexico: McGraw-Hill, 1998.

[21] Schackelford, J., Ciencia de materiales para ingenieros. Mexico: Pearson, 1995.

[22] Dunne, F. and Petrinic, N., Introduction to computational plasticity. Oxford: Oxford University Press, 2005.

[23] Gordon, J., Estructuras o porque las cosas no se caen. Buenos Aires: CALAMAR Ediciones, 2004.

[24] Hartmann, S., Kontaktanalyse dünnwandiger Strukturen bei großen Deformationen,: PhD. Thesis, Institut für Baustatik und Baudynamik, Universität Stuttgart, Germany, 2007.

G. J. Torrente-Prato, received the BSc. Eng in Material Engineering in 2000, the MSc. degree in Material Engineering in 2004, and the PhD degree in Engineering in 2009, all of them from Simon Bolivar University, Venezuela. Since 2009 he is professor of the Mechanical Department at Simon Bolivar University. His research interests include: simulation and modeling of fluids and solids, forming processes and thermal plasma processing.
ORCID: /0000-0003-1237-3077

UNIVERSIDAD **NACIONAL** DE COLOMBIA

SEDE MEDELLÍN

FACULTAD DE MINAS

Área Curricular de Ingeniería
Geológica e Ingeniería de Minas y Metalurgia

Oferta de Posgrados

Especialización en Materiales y Procesos
Maestría en Ingeniería - Materiales y Procesos
Maestría en Ingeniería - Recursos Minerales
Doctorado en Ingeniería - Ciencia y Tecnología de Materiales

Mayor información:

E-mail: acgeomin_med@unal.edu.co
Teléfono: (57-4) 425 53 68